

## 7 Perception of Deformable Objects and Compliant Manipulation for Service Robots

Jörg Stückler and Sven Behnke

University of Bonn, Computer Science Institute VI, Autonomous Intelligent Systems

**Abstract** We identified softness in robot control as well as robot perception as key enabling technologies for future service robots. Compliance in motion control compensates for small errors in model acquisition and estimation and enables safe physical interaction with humans. The perception of shape similarities and deformations allows a robot to adapt its skills to the object at hand, given a description of the skill that generalizes between different objects. In this chapter, we present our approaches to compliant control and object manipulation skill transfer for service robots. We report on evaluation results and public demonstrations of our approaches.

### 7.1 Introduction

In today's industrial settings, robots are frequently required to execute motions fast, precisely, and reliably. The use of high-stiffness motion control can guarantee robust operation in this domain, but it also demands precise models of the dynamics of the robot mechanism and the manipulated objects. Furthermore, precautions need to be taken to prevent physical interaction with humans under any circumstances. This approach may not be applicable, e.g., in human-robot collaborative scenarios, in less structured environments, or when physical interaction with humans is unavoidable.

Generalization of robot skills is a further aspect that needs to be considered to bring robots into new applications. Often in practice, manipulation controllers need to be manually designed for each specific instance of an object class. This approach limits the range of possible applications of robotics technology by the effort that has to be taken to adapt the robot to the task, especially for service robots in our everyday environments.

We identified softness in robot control as well as robot perception as key enabling technologies for future service robots. Compliance in motion control compensates for small errors in model acquisition and estimation and enables safe physical interaction with humans. The perception of shape similarities and deformations allows a robot to adapt its skills to the object at hand, given a description of the skill that generalizes between different objects.

In this chapter, we present our approaches to compliant control and object manipulation skill transfer for service robots. We propose compliant task-space control for redundant manipulators driven by servo actuators. The actuators in our approach are back-drivable and allow for configuring the maximum torque used for position control. From differential inverse kinematics, we derive a method to limit the torque of the joints depending on how much they contribute to the achievement of the motion in task-space. Furthermore, our approach not only allows for adjusting compliance in the null-space of the motion but also in the individual dimensions in task-space. This is very useful when only specific dimensions in task-space shall be controlled in a compliant way. We utilize this compliance in several applications that require physical human-robot interaction. For instance, we demonstrate the cooperative carrying of a large object. We also use compliant control when handing objects to a human, or to guide the robot at its hand.

In many object manipulation scenarios, controllers can be described for specific object instances through grasp poses and 6-DoF trajectories relative to the functional parts of the objects. One can pose the problem of skill transfer as establishing correspondences between the object shapes, i.e., between the functional parts. Grasps and motions are then transferrable to novel object instances according to the shape deformation. We propose an efficient deformable registration method that provides a dense displacement field between object shapes observed in RGB-D images. From the displacements, local transformations can be estimated between points on the object surfaces. We apply these local transformations to transfer grasps and motion trajectories between the objects.

We develop our approaches with our service robots Cosero and Dynamaid [12,14,15]. The human-scale robots are equipped with two anthropomorphic arms each on upper bodies that can be moved on a linear actuator in the vertical direction in order to manipulate on different height levels. They move in indoor environments on omnidirectional drives with small footprints. A communication head provides the robots with human-like appearance for natural human-robot interaction. Light-weight design facilitates inherent safety of the robots.

## ***7.2 Compliant Control for Service Robots***

Task-space motion control, initially developed by Liegeois [4], is a well-established concept in robotics (see [6] for a recent survey). Common to task-space control methods is to transfer motion specified in a space relevant to a task to joint-space motion. One simple example is the control of the end-effector of a serial kinematic chain along pose trajectories in Cartesian space. For compliant motion control in task-space, acceleration- and force-based methods are frequently employed. We propose a velocity-based method. Instead of relying on redundancy resolution for compliant control, we adjust compliance for each dimension and di-

rection in task-space as well as in the null-space of the motion when the robot kinematics is redundant for the task.

Using such compliant control, we implemented several service robot tasks that require soft and compliant interaction with objects or persons. One such task is the cooperative transport of large objects by a robot and a person. Khatib et al. [2] investigated manipulation of large objects with multiple mobile manipulators. This approach requires exact identification of the dynamics of the mobile manipulators. Yokoyama et al. [17] use an HRP2 humanoid robot to carry a large panel together with a human. The robot finds the panel by stereo vision through a model-based recognition system. The walking direction of the robot is controlled by voice commands and by force-torque sensors on the robot wrist. In our approach, the robot also recognizes the intention of the person through the motion of the table. Instead of specific force-torque sensing in the wrist, we apply compliance control to let the human move the robot's end-effectors through the table.

A further application of compliant control which we have investigated is the problem of robot guidance by a human through physical interaction. Christensen et al. [1] proposed to lead a domestic service robot around the house for initial map acquisition by taking its hand. The higher bandwidth of the arm allows for decoupling the applied forces from the robot motion. Oudeyer et al. [7] report on such following behavior emerging from compliant whole-body control of a humanoid robot. In our work, we couple compliant control of the arms with the laser-scanner based perception of the human guide.

### 7.2.1 Compliant Task-Space Control

We employ velocity-based task-space control and derive a control law for compliant motion of the arms. We assume that the robot actuators follow position trajectories through torque control. In our approach, we assume that the torque applied by the actuator can be limited. We derive the responsibility of each joint for the motion in task-space, and distribute a desired maximum torque onto the involved joints according to their responsibility.

Central to task-space controllers is a mapping from joint states  $q \in \mathbf{R}^m$  to states  $x \in \mathbf{R}^n$  in task-space, i.e., the forward kinematics  $x = f(q)$ . Inversion of the linearized relationship yields a mapping from task-space velocities to joint-space velocities  $\dot{q} \approx J^T \dot{x} + (I - J^T J) \dot{q}^0$ , in which secondary joint motion  $\dot{q}^0$  can be projected into the null-space of the mapping such that the tracking behavior in task-space is not altered.

Given a desired trajectory in task-space  $x_d(t)$ , we derive a control scheme to follow the trajectory with a position-controlled servo actuator

$$\dot{x}(t) = K_x (x_d(t) - x(t)), \quad \dot{q}(t) = K_q \left( J^\dagger \dot{x}(t) + \alpha (I - J^\dagger J) \nabla g(q(t)) \right),$$

where  $K_x$  and  $K_q$  are gain matrices. The cost function  $g(q(t))$  optimizes secondary criteria in the null-space of the motion, and  $\alpha$  is a step-size parameter. Cost criteria typically include joint limit avoidance or the preference of a convenient joint state.

We set a compliance  $c \in [0, 1]^n$  in linear dependency of the deviation of the actual state from the target state in task-space, such that the compliance is one for small displacements, zero for large ones, and linearly interpolates in between. For each task dimension, the motion can be set compliant in the positive and the negative direction separately, allowing e.g. for being compliant in upward direction, but stiff downwards. If the task dimension is not set compliant, we wish to use high holding torques  $\tau_i^x$  to position-control this dimension. If it is set compliant, the maximal holding torque interpolates between a minimal value for full compliance and a maximum torque for zero compliance.

To implement compliant control, we measure the responsibility of each joint for the task-space motion through the inverse of the Jacobian

$$R_{task}(t) := abs \left[ J^\dagger(q(t)) \begin{pmatrix} \dot{x}_1(t) & 0 & \cdots & 0 \\ 0 & \dot{x}_2(t) & \ddots & \vdots \\ \vdots & \ddots & \ddots & 0 \\ 0 & \cdots & 0 & \dot{x}_n(t) \end{pmatrix} \right],$$

where abs determines absolute values of a matrix element-wise.

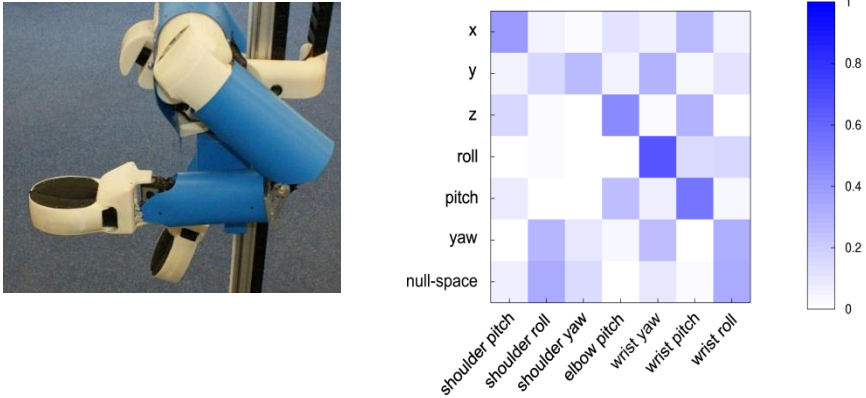


**Fig. 7.1** Activation matrix in compliant control. Task-space dimensions correspond to forward/backward (x), lateral (y), vertical (z), and rotations around the axes (roll, pitch, yaw).

Each entry  $(i, j)$  of the matrix measures the contribution of the velocity of the  $j$ -th task component to the velocity of the  $i$ -th joint. In addition, we also define the responsibility of each joint for the null-space motion  $R_0(t) := \text{abs}[\alpha(I - J^T J)\nabla g(q(t))]$ . To finally distribute our desired torque limits, we determine an activation matrix  $A(t)$  by normalizing the responsibility of the joints to sum to one along each task dimension. Fig. 7.1 shows an example matrix. The task-component maximal torques are then distributed according to the activation of each joint, i.e.  $\tau_q = A(t)\tau_x$ .

## 7.2.2 Applications of Compliant Control in Everyday Environments

### Object Hand-Over to a Person

Object hand-over from a robot to a person can be implemented with several strategies. For instance, object release could be triggered by speech input or by specialized sensory input such as distance or touch sensors. Through compliant control, we establish a very natural way of hand-over by simply releasing the object when the interaction partner pulls on the object (see Fig. 7.2, left). To implement this, the robot offers the object to the person and controls the motion of its end-effector compliant in forward, in upward direction, and in pitch rotation. The robot releases the object when it detects a significant displacement of its end-effector.

### Guiding a Robot at its Hand

Taking the robot by its hand and guiding it is a simple and intuitive mean to communicate locomotion intents to the robot (see Fig. 7.3, left). We combine person perception with compliant control to implement such behavior: the robot extends one of its end-effectors forward and waits for the user. As soon as the user appears in front of the robot and exerts forces on the end-effector, the robot starts to follow the motion of the end-effector by driving in translational directions. The robot avoids the guide with a potential field method. It rotates its base to keep the guide at a constant angle, relative to its heading direction.

### Cooperative Carrying of a Table

Cooperative transportation of large objects is a typical collaborative task in which multiple persons or robots physically interact to solve a task (Fig. 7.2 right).



**Fig. 7.2** Left: Cognitive service robot Cosero hands an object to a person. Right: cooperative carrying of a table by a person and Cosero.

We demonstrate object perception, person awareness, and compliant control in the task of cooperatively carrying a table by a person and a robot. As soon as the person appears in front of the robot, the robot approaches the table, grasps it, and waits for the person to lift it. After the robot visually perceives the lifting of the table, it also lifts the table and starts to follow the motion of the person. It sets the motion of the end-effectors compliant in the sagittal and lateral direction, and in yaw orientation. By this, the robot complies when the person pulls and pushes the table. The robot follows the motion of the person by controlling its omnidirectional base to realign the hands to the initial grasping pose with respect to the robot. The person may cease the carrying of the table at any time by lowering the table, which is also visually perceived by the robot.

### Manipulation of Articulated Objects

We apply compliant control to the opening and closing of doors that can be moved without the handling of an unlocking mechanism (see Fig. 7.3, right). To open a door, our robot drives in front of it, detects the door handle with its torso laser, approaches the handle, and grasps it. The drive moves backward while the gripper moves to a position to the side of the robot in which the opening angle of the door is sufficiently large to approach the open fridge or cabinet. The gripper follows the motion of the door handle through compliance in the lateral and the yaw directions. The robot moves backward until the gripper reaches its target position. For closing a door, the robot has to approach the open door leaf, grasp the handle, and move forward while it holds the handle at its initial grasping pose relative to the robot. When the arm is pulled away from this pose by the constraining motion of the door leaf, the drive corrects for the motion to keep the handle at its initial pose relative to the robot. The closing of the door can be detected when the arm is pushed back towards the robot.



**Fig. 7.3** Left: A person guides Cosero at its hand. Right: Dynamaid opens and closes a refrigerator using compliant control at RoboCup 2010 in Singapore.

### 7.2.3 Public Demonstrations

The tracking behavior of our compliant control method has been extensively evaluated in our prior work in [10]. In general, our approach exhibits good tracking performance in compliant mode in linear and rotational directions. If gravity needs to be compensated, a compliant motion orthogonal to the gravity direction may be slightly less accurate due to the fact that joints are involved in both counteracting gravity as well as moving into the compliant direction.

We demonstrated the applications of compliant control described in Sec. 7.2.2 with our service robot Cosero publicly at several occasions at RoboCup@Home competitions. Object hand-over occurs very frequently in the test scenarios of the competition. Our approach leads to a very natural and intuitive robot behavior that is well understood by users and has high success rates. We have demonstrated the opening and closing of a refrigerator in the final demonstration of the @Home league at RoboCup 2010 in Singapore<sup>2</sup>. The cooperative carrying of a table was first shown in the finals at RoboCup 2011 in Istanbul, Turkey<sup>3</sup>. It was also shown in combination with guiding the robot to the location of the table at RoboCup German Open in 2013. The demonstrations have been important aspects for convincing the juries of our open demonstrations and finals. We won the international RoboCup@Home competitions in 2011 [15], 2012 [14], and 2013 [12]. We also achieved 1<sup>st</sup> place in the league at RoboCup German Open competitions from 2011 to 2014.

<sup>2</sup> [https://www.youtube.com/watch?v=TObo4\\_N0AAQ](https://www.youtube.com/watch?v=TObo4_N0AAQ)

<sup>3</sup> <https://www.youtube.com/watch?v=nG0mJiODrYw>

### 7.3 Object Manipulation Skill Transfer

Our approach to skill transfer can be seen as a variant of learning from demonstration. Recently, Schulman et al. [8] proposed an approach in which motion trajectories are transferred between shape variants of objects. They primarily demonstrate tying knots in rope [8] and suturing [9], while they also show examples for folding shirts, picking up plates, and opening a bottle. Their non-rigid registration method is a variant of the thin plate spline robust point matching (TPS-RPM) algorithm. We develop an efficient deformable registration method based on the coherent point drift method (CPD [5]) to align RGB-D images efficiently and accurately. We demonstrate bimanual tool-use, and propose to select tool end-effectors as reference frames for the example trajectory, where it is appropriate. In contrast to the method in [8,9], we do not assume the estimated displacement field to be valid at any pose on the motion trajectory. Instead, we design example motions relative to reference frames. These reference frames are transformed between example and new object.

#### 7.3.1 Efficient RGB-D Deformable Registration

We propose a multi-resolution extension to the coherent point drift (CPD [5]) method to efficiently perform deformable registration between RGB-D images (see Fig. 7.4, top). Instead of processing the dense point clouds of the RGB-D images directly with CPD, we utilize multi-resolution surfel maps (MRSMaps<sup>4</sup> [13]) to perform deformable registration on a compressed image representation. This image representation stores the joint color and shape statistics of points within 3D voxels (coined surfels) at multiple resolutions in an octree. The maximum resolution at a point is limited proportional to its squared distance in order to capture the error properties of the RGB-D camera. In effect, the map exhibits a local multi-resolution structure which well reflects the accuracy of the measurements and compresses the image from 640×480 pixels into only a few thousand surfels.

The CPD method assumes a displacement field  $v: Y \rightarrow X$  between a model point set  $Y$  and the scene points  $X$ . It aims at minimizing the squared error of the deformed points in  $Y$  with their counterparts in  $X$ ,

$$\ln p(X, v | \sigma) = \ln p(X | \sigma, v) - \lambda/2 \|v\|_H^2.$$

By introducing a norm on the displacement field in a reproducing kernel Hilbert space  $H$ , smoothness can be enforced. The regularized objective has a closed-form solution given the assignment of points, which requires solving a system of linear equations whose size is quadratic in the number of model points. Instead of

---

<sup>4</sup> Our MRSMap implementation is available open-source from <http://code.google.com/p/mrsmap/>.



assuming a one-to-one mapping between the points, the CPD method explains the deformed points in  $Y$  as samples from a mixture model, in which each sample in  $X$  is a Gaussian mixture component. Since the assignment probabilities between the point sets are not known a-priori, the probabilities and the displacement field are recovered iteratively through expectation-maximization.

Color and contours in the depth image are integrated as additional point dimensions. We process RGB-D images from coarse to fine resolutions in our MRSSMap representation. Since the volume covered shrinks with resolution, we constrain the borders of a fine resolution to the coarser resolution result. This objective also has a closed-form solution for the displacement field. Finally, to improve robustness and to facilitate the linear systems to be sparse, we use a compact support kernel.

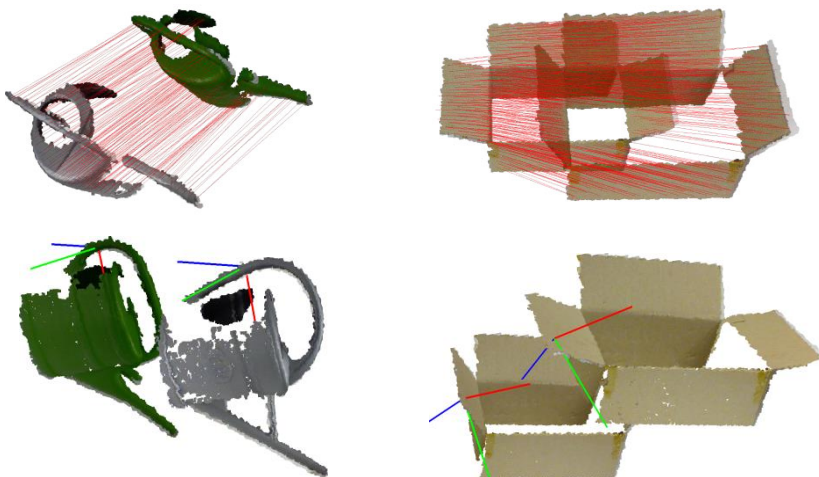
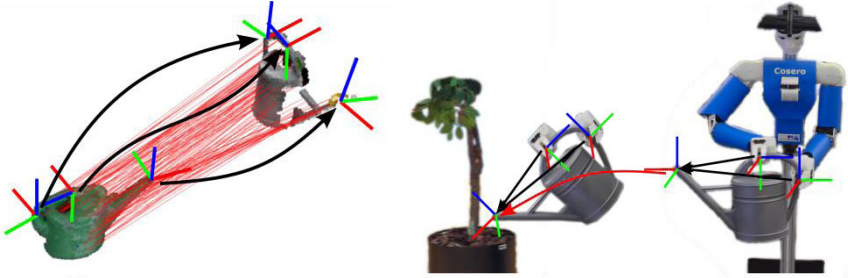


Fig. 7.4 Top: deformable registration examples. Bottom: local transformation examples.

### 7.3.2 Skill Transfer through Shape Matching

We describe object manipulation skills as grasp poses and motion trajectories relative to an object (see Fig. 7.5). We exploit that often shape deformations induce correspondences in the functional parts between objects of the same functional object class. When the robot observes a new kind of object of a class that it knows to handle, it matches the shapes of the object at hand with the known object, and transfers grasps and motions to the new one. To this end, we apply our deformable registration method. We define grasp poses and motion trajectories in terms of local coordinate frames relative to the object's reference frame. Hence, we need a



**Fig. 7.5** Skill transfer. Left: We transfer grasp and tool end-effector poses between objects through deformable registration. Right: We represent skills as motions of the tool end-effector relative to other objects, which can be transferred once the tool end-effector of a new object is known. The motion of the tool end-effector induces a motion of the grasps.

method for estimating local coordinate frame changes between the observed object and the known object.

We estimate the local coordinate frame changes from the displacement field that is recovered with our deformable registration method (see Fig. 7.4, bottom). The infinitesimal deformation at a point  $y$  is specified by the Jacobian of the displaced point,  $\nabla\varphi(y) = I + \nabla v(y)$ . The local rotation  $R$  is obtained through polar decomposition of the Jacobian  $\nabla\varphi(y) = RU$ .

### 7.3.3 Results

We have evaluated accuracy and run-time of our deformable registration method and compared it with plain processing of RGB-D images using CPD. On synthetically deformed RGB-D images, we achieve an average run-time of 1.29 s, plain processing requires 4.74 s. Our method also is more accurate: in average our method has a low deviation of 0.0178 m from the ground truth displacements, while plain processing yields 0.0482 m mean error. Note that for plain image processing, the original images had to be subsampled from  $640 \times 480$  to  $80 \times 60$  resolution. Further evaluation results can be found in [11].

We publicly demonstrated object manipulation skill transfer based on our deformable registration approach during the @Home league Open Challenge at RoboCup 2013 in Eindhoven, Netherlands<sup>5</sup>. The jury chose one of two new cans, while the skill was pretrained for a third instance of cans. Our robot Cosero transferred watering can manipulation skills to a novel can. Fig. 7.6 shows images taken during the demonstration. The demonstration was well received by the jury consisting of team leaders and received high scores, which was an important contribution to winning the 2013 RoboCup@Home competition.

<sup>5</sup> <http://www.youtube.com/watch?v=I1kN1bAeeB0>

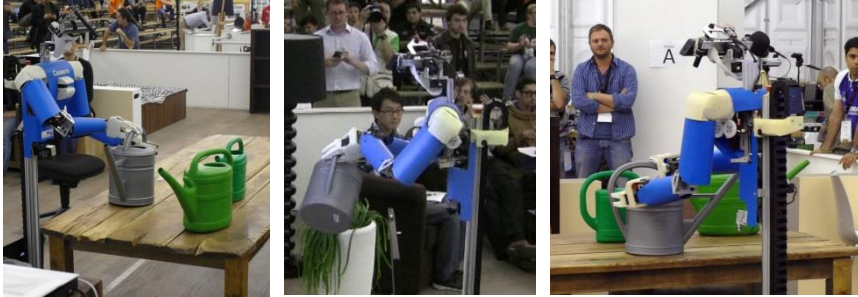


**Fig. 7.6** Cosero transfers the bi-manual skill of watering a plant to a novel watering can in the final RoboCup@Home demonstration at RoboCup 2013 in Eindhoven.

## 7.4 Conclusions

In this chapter, we presented our approaches to compliant control and deformable registration that enable soft interaction with objects and persons, and that increase the flexibility of robot behavior in everyday environments.

We developed compliant control for the anthropomorphic arms of our service robots Cosero and Dynamaid. It has been used to demonstrate a variety of tasks in everyday environments that either require soft manipulation of objects such as opening and closing doors, or soft physical interaction with humans. For transferring object manipulation skills, we developed an efficient deformable registration method for RGB-D images. It allows for transferring grasp poses and tool end-effectors between shape variants of functional types of objects. In a public demonstration, Cosero showed bimanual handling of a novel watering can to water a plant. The reported public demonstrations have been key contributions to winning the German and international RoboCup@Home competitions since 2011.

In future work, we want to further study the modelling and manipulation of deformable objects. Through compliant control, interactive learning of deformable object models can be made possible.

## 7.5 References

- [1] Christensen HI, Hüttenrauch H, Severinson-Eklundh K (2000) Human-Robot Interaction in Service Robotics. In: Proc of Robotik
- [2] Khatib O, Yokoi K, Chang K, Ruspini D, Holmberg R, Casal A, Baader A (1996) Force strategies for cooperative tasks in multiple mobile manipulation systems. In: Proc of ISRR, 333-342
- [3] Khatib O (1988) Object manipulation in a multi-effector robot system. In: Proc. of International Symposium of Robotic Research (ISRR), 137-144

- [4] Liegeois A (1977) Automatic Supervisory Control of the Configuration and Behavior of Multibody Mechanisms. *IEEE Transactions on Systems, Man and Cybernetics* 7(12):868-871
- [5] Myronenko A, Song X (2010) Point set registration: coherent point drift. *IEEE Trans on PAMI* 32(12):2262-2275
- [6] Nakanishi J, Cory R, Mistry M, Peters J, Schaal S (2008) Operational Space Control: A Theoretical and Empirical Comparison. *Int Journal of Robotics Research* 27(6):737-757
- [7] Oudeyer P-Y, Ly O, Rouanet P (2011) Exploring robust, intuitive and emergent physical human-robot interaction with the humanoid robot Acroban. In: *Proc of the IEEE-RAS Int Conf on Humanoid Robots*
- [8] Schulman J, Gupta A, Venkatesan S, Tayson-Frederick M, Abbeel P (2013) A case study of trajectory transfer through non-rigid registration for a simplified suturing scenario. In: *Proc of IEEE/RSJ Int Conf on Intelligent Robots and Systems (IROS)*
- [9] Schulman J, Ho J, Lee C, Abbeel P (2013) Learning from demonstrations through the use of non-rigid registration. In: *Proc of the 16th Int Symposium on Robotics Research (ISRR)*
- [10] Stückler J, Behnke S (2012) Compliant Task-Space Control with Back-Drivable Servo Actuators. In: *RoboCup 2011, LNCS 7416, 78-89*
- [11] Stückler J, Behnke S (2014) Efficient Deformable Registration of Multi-Resolution Surfel Maps for Object Manipulation Skill Transfer. In: *Proc of IEEE Int Conf on Robotics and Automation (ICRA)*
- [12] Stückler J, Droeschel D, Gräve K, Holz D, Schreiber M, Topalidou-Kyniazopoulou A, Schwarz M, Behnke S (2014) Increasing Flexibility of Mobile Manipulation and Intuitive Human-Robot Interaction in RoboCup@Home. In: *RoboCup 2013, LNCS 8371, 135-146*
- [13] Stückler J, Behnke S (2014) Multi-resolution surfel maps for efficient dense 3D modeling and tracking. *Journal of Visual Communication and Image Representation* 25(1):137-147
- [14] Stückler J, Badami I, Droeschel D, Gräve K, Holz D, McElhone M, Nieuwenhuisen M, Schreiber M, Schwarz M, Behnke S (2013) NimRo@Home: Winning Team of the RoboCup-@Home Competition 2012. In: *RoboCup 2012, LNCS 7500, 94-105*
- [15] Stückler J, Holz D, Behnke S (2012) RoboCup@Home: Demonstrating Everyday Manipulation Skills in RoboCup@Home. *IEEE Robotics & Automation Magazine* 19(2):34-42
- [16] Williams D, Khatib O (1993) The virtual linkage: A model for internal forces in multi-grasp manipulation. In: *Proc of the IEEE Int. Conf. on Robotics and Automation (ICRA)*
- [17] Yokoyama K, Handa H, Isozumi T, Fukase Y, Kaneko K, Kanehiro F, Kawai Y, Tomita F, Hirukawa H (2003) Cooperative works by a human and a humanoid robot. In: *Proc of IEEE Int Conf on Robotics and Automation (ICRA), 2985-2991*